

Introducing a photo-switchable azo-functionality inside Cr-MIL-101-NH₂ by covalent post-synthetic modification†Antje Modrow,^a Dordaneh Zargarani,^b Rainer Herges^b and Norbert Stock^{*a}

Received 23rd March 2012, Accepted 20th May 2012

DOI: 10.1039/c2dt30672g

For the first time an azo functionality was covalently introduced into a MOF by post-synthetic modification. The reaction of Cr-MIL-101-NH₂ with *p*-phenylazobenzoylchloride (**1**) and 4-(phenylazo)-phenylisocyanate (**2**) as the reactants led to the compounds Cr-MIL-101_amide and Cr-MIL-101_urea, with the azo groups protruding into the mesoporous cages. XRPD and N₂ sorption measurements confirm the intactness of the framework and the successful covalent modification was proven by IR- and NMR-spectroscopy. Furthermore, *cis/trans* isomerisation upon irradiation with light was demonstrated by UV/Vis spectroscopy. More distinct changes in the UV/Vis spectra were observed for Cr-MIL-101_amide compared to Cr-MIL-101_urea, while the degree of functionalization, *i.e.* the number of reacted NH₂-groups, seems to have a less pronounced effect. The variation of the sorption properties due to the *cis/trans* isomerisation was proven by methane adsorption measurements.

Introduction

The synthesis and characterization of metal–organic frameworks (MOFs) have attracted considerable interest in recent years, because of their potential applications in catalysis, drug delivery, gas separation and storage.^{1–6} One of the most attractive features of MOFs, compared to zeolites, is their even higher structural variability.⁷ MOFs are built up from inorganic building blocks which are bridged by organic linker molecules.⁸ Because of the modular assembly, the pore size, -window and -shape can be adjusted by choosing different linker molecules, which often do not influence the overall crystal structure.^{9,10} The synthesis of these compounds can be accomplished under various reaction conditions.¹¹

It is also possible to introduce additional functionalities inside the MOF. This can be achieved by choosing an already functionalized linker molecule^{12,13} or by post-synthetic modification (PSM).^{14,15} Since normally MOFs are synthesized in a solvo-thermal reaction, the usage of a functionalized linker molecule is limited, because the solubility and reactivity are changed or different crystal structures are obtained. Nevertheless, some examples of isoreticular MOFs containing linker molecules of different sizes and/or containing functional groups have been reported in the literature.^{16–19} For larger or more reactive functional groups the direct incorporation is not feasible.¹⁵ In some

cases this can be achieved by post-synthetic modification of the MOF. In principle, three different ways are used for the functionalisation: (1) functional groups (*e.g.* –NH₂, –NO₂, –N₃) react with another reactive molecule inside the pores,^{20–24} (2) coordinative unsaturated sites are used,²⁵ and (3) nucleophilic substitution takes place at the aromatic ring.²⁶

Important requirements for the post-synthetic modification are a high chemical stability and large, accessible pores of the host material. A good candidate for post-synthetic modification is Cr-MIL-101-NH₂ [Cr₃(μ₃O)(OH)(H₂O)₂(O₂CC₆H₄CO₂)₃]*n*H₂O due to its high specific surface area, large, accessible pores and chemical as well as thermal stability. Recently, the successful post-synthetic modification with ethyl isocyanate was shown.²⁶

Post-synthetic modification can also be initiated by light. By employing *trans*-1,2-bis(4-pyridyl)ethane (bpe)²⁷ or 1,4-bis-[2-(4-pyridyl)ethenyl]benzene (bpeb)²⁸ for the MOF-synthesis two compounds were obtained, which could be post-synthetically modified by a single-crystal to single-crystal light-driven reaction.

Introducing a photo-switchable functional group, light can be used to reversibly modify the structure. This has been demonstrated by using azobenzene-functionalized dye molecules as linker molecules, *i.e.* azophenylbipyridine,¹² azophenylterephthalic acid²⁹ or azophenylimidazole.¹³ Azobenzene derivatives are the molecules of choice since their *cis/trans* isomerisation is controlled by light and this class of photochromic compound has been thoroughly investigated.^{30–32} The thermodynamically stable *trans*-isomer can be switched by irradiation with UV light ($\lambda = 365$ nm) to the *cis*-isomer. The back switching can be achieved by irradiation with visible light ($\lambda = 455$ nm) or thermally. The *cis/trans* isomerisation of the azo group leads to changes in the geometry of the molecule, which were evidenced by X-ray powder diffraction measurements in

^aInstitut für Anorganische Chemie, Christian-Albrechts-Universität, Max-Eyth-Straße 2, D-24118 Kiel, Germany.

E-mail: stock@ac.uni-kiel.de; Fax: (+49) 0431-880-1775;

Tel: (+49) 0431-880-1675

^bOtto-Diels-Institut für Organische Chemie, Christian-Albrechts-Universität, Otto-Hahn-Platz 4, D-24098 Kiel, Germany

†Electronic supplementary information (ESI) available. See DOI: 10.1039/c2dt30672g

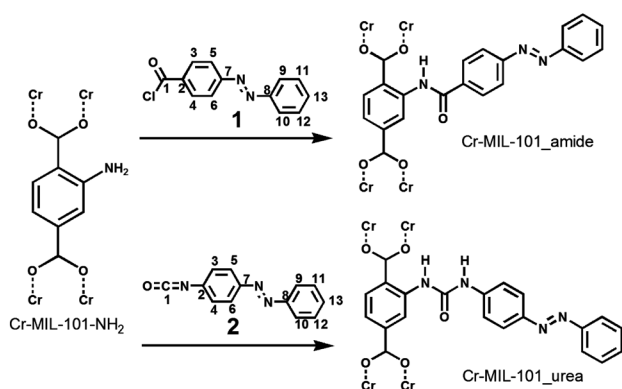


Fig. 1 Post-synthetic modification of Cr-MIL-101-NH₂ with *p*-phenylazobenzoylchloride (**1**) and 4-(phenylazo)phenylisocyanate (**2**).

the case of Zn-CAU-5.¹² The change of the polarity, dipole moment and required space leads to differences in the sorption behaviour.²⁹

Here, we present the post-synthetic modification of Cr-MIL-101-NH₂ with *p*-phenylazobenzoylchloride (**1**) and 4-(phenylazo)phenylisocyanate (**2**) to yield Cr-MIL-101_{amide} and Cr-MIL-101_{urea}, respectively (Fig. 1). The influence of the degree of functionalisation on the reversible *cis/trans* isomerisation of the covalent attached azobenzene derivatives was investigated using UV/Vis spectroscopy as well as methane gas adsorption measurements.

Experimental

Materials

The chemicals 4-aminoazobenzene (ABCR), phosgene (20% toluene, Sigma Aldrich), toluene (Merck), CrCl₃ (Sigma Aldrich), nitroterephthalic acid (Sigma Aldrich), and SnCl₂·2H₂O (Merck) were obtained commercially and used as received.

Synthesis of *p*-phenylazobenzoylchloride (**1**)

p-Phenylazobenzoylchloride was synthesized in a two-step reaction as described in the literature.³³ The purity of the compound was confirmed by ¹H-NMR and ¹³C-NMR spectroscopy.

¹H-NMR (220 MHz, DMSO, 300 K, TMS, numbering according to Fig. 1): δ = 8.16 (d, 2H, *H*-3, *H*-4), 7.97 (d, 2H, *H*-5, *H*-6), 7.51 (d, 2H, *H*-9, *H*-10), 7.63 (m, 3H, *H*-11, *H*-12, *H*-13) ppm.

¹³C-NMR (500 MHz, DMSO-d₆, numbering according to Fig. 1): δ = 167.1 (s, *C*-1), 154.7 (s, *C*-7), 152.4 (s, *C*-8), 133.3 (s, *C*-2), 132.7 (s, *C*-13), 131.1 (s, *C*-3, *C*-4), 130.0 (s, *C*-11, *C*-12), 123.3 (s, *C*-5, *C*-6), 123.0 (s, *C*-9, *C*-10) ppm.

Synthesis of 4-(phenylazo)phenylisocyanate (**2**)^{34,35}

4-(Phenylazo)phenylisocyanate was synthesized starting from phosgene and 4-aminoazobenzene. In a three-necked flask, 20 mL phosgene solution (20% in toluene) was cooled at -10 °C. 2.48 g 4-Aminoazobenzene were dissolved in 50 mL

dry toluene and added dropwise into the cooled phosgene. While adding 4-aminoazobenzene, the colour changed immediately from orange to dark red-brown. The reaction mixture was stirred for 1 h at -10 °C and afterwards at room temperature (24 °C) for about 45 min. The flask was equipped with a condenser (-20 °C) and the reaction mixture was refluxed at 100 °C. After 30 min, HCl bubbles were observed in the oil trap and the reaction mixture turned dark. After 5 h the reaction mixture was cooled to room temperature and filtered. The filtrate was treated with N₂ gas for 45 min to remove phosgene. The toluene was evaporated under reduced pressure and about 1.12 g orange crystals of 4-(phenylazo)phenylisocyanate were obtained. The purity of the compound was confirmed by ¹H-NMR and ¹³C-NMR spectroscopy.

¹H-NMR (220 MHz, DMSO-d₆, 300 K, TMS, numbering according to Fig. 1): δ = 7.9 (dd, 4H, *H*-5, *H*-6, *H*-9, *H*-10), 7.5 (m, 3H, *H*-11, *H*-12, *H*-13), 7.2 (d, 2H, *H*-3, *H*-4) ppm.

¹³C-NMR (500 MHz, DMSO-d₆, numbering according to Fig. 1): δ = 152.5 (s, *C*-6), 150.2 (s, *C*-7), 135.9 (s, *C*-12), 131.2 (s, *C*-1), 129.1 (s, *C*-3), 129.1 (s, *C*-3), 125.4 (s, *C*-13), 125.3 (s, *C*-10, *C*-11), 124.3 (s, *C*-8, *C*-9), 122.9 (s, *C*-4, *C*-5) ppm.

Synthesis of Cr-MIL-101-NO₂

Cr-MIL-101-NO₂ was synthesized in a hydrothermal reaction of 211 mg (1 mmol) nitroterephthalic acid and 266 mg (1 mmol) CrCl₃ in 5 mL H₂O at 180 °C for 96 h. The green product was centrifuged and transferred into a microwave vessel (Biotage, 10–20 mL) with EtOH. The vessel was heated for 30 min at 150 °C in the microwave. The green product was centrifuged and dried.

Synthesis of Cr-MIL-101-NH₂

Cr-MIL-101-NH₂ was synthesized in a 6 h reaction at 80 °C from 100 mg (0.148 mmol) Cr-MIL-NO₂ and 700 mg (3 mmol) SnCl₂·2H₂O in 30 mL absolute EtOH.²⁶ The mixture was cooled to room temperature, 10 mL concentrated HCl were added and the mixture was stirred overnight. The mixture was centrifuged and the solid was washed several times with H₂O and EtOH.

Post-synthetic modification

For each PSM reaction, 80 mg (0.36 mmol NH₂-groups) Cr-MIL-101-NH₂ were placed in a microwave vial (2–5 mL, Biotage) and activated overnight in an isothermal oven at 80 °C. Afterwards the sample was evacuated for about 1 h at 10⁻² kPa. The dye was dissolved in 2 mL dry acetonitrile and the solution was injected through a septum. The microwave vial was vented with air, sealed and placed in the microwave oven (Biotage, Initiator) for 3 h at 130 °C. The mixture was centrifuged and washed thoroughly with EtOH until the EtOH was colourless. For the reactions with dye molecule **2** all steps were carried out under a N₂ atmosphere. Four different molar ratios were used (Table 1).

NMR measurements. All Cr-MIL-101 samples were decomposed with NaOH after the post-synthetic modification

Table 1 Molar ratios and amounts of reactants used in the PSM reactions. The amount of Cr-MIL-101-NH₂ was kept constant (80 mg, which corresponds to 0.36 mmol –NH₂ groups)

Molar ratio NH ₂ : dye	Dye [mmol]	Dye 1 [mg]	Dye 2 [mg]
2 : 1	0.18	44	40
1.5 : 1	0.24	59	54
1 : 1	0.36	88	80
1 : 2	0.71	174	158

reaction.²⁶ Precipitated Cr(OH)₃ was removed by filtration. Afterwards HCl was added to the yellow solution and an orange (dye molecule **1**) or red (dye molecule **2**) precipitation was obtained after centrifugation. The precipitated solids were only soluble in dimethylsulfoxide (DMSO), therefore all NMR spectra were recorded in DMSO-d₆. All NMR-measurements were performed using a Bruker FT-NMR-spectrometer, Avance 600 (¹H: 600 MHz; ¹³C: 150 MHz).

XRPD measurements. All XRPD measurements were carried out in transmission mode using a STOE high-throughput powder diffractometer equipped with an image-plate position-sensitive detector (IPPSD).

IR-measurements. All IR-measurements were performed with a Bruker ALPHA-FT-IR spectrometer.

Sorption measurements. All samples were activated *in vacuo* (10⁻² kPa) at 140 °C for 6 h before the sorption measurements. The measurements were carried out with a BELSORP-Max apparatus from BEL Japan Inc.

UV/Vis measurements. All UV/Vis spectra of the modified Cr-MIL-101-NH₂ samples were carried out in a BaSO₄ matrix and measured in reflection geometry. Therefore, 3 mg of the respective compound were ground with 150 mg BaSO₄. The UV/Vis spectra were converted into absorption spectra using the Kubelka–Munk equation. All UV/Vis measurements were performed with a Cary 5000 from Varian.

Switching experiments. For all switching experiments two different LED light sources from NICHIA were used. UV light was obtained from a LED of 365 nm (NC4U122E), visible light was obtained from a LED of 455 nm (NS6C083A). For the UV/Vis switching experiments the sample was mixed with BaSO₄ and transferred into the sample holder. After the first measurement, the sample holder was irradiated with UV light and a UV/Vis spectrum was recorded again. The back switching was achieved by irradiation of the sample holder with visible light or by placing the sample holder in the dark for 16 h before a UV/Vis spectrum was recorded.

Methane adsorption measurements. Before the first measurement at 298 K was carried out, the samples were activated at 140 °C for 6 h. *Cis/trans* isomerisation was achieved at room temperature under vacuum (~0.1 mbar). The samples were irradiated for 90 min in the quartz glass sorption sample holders which were connected the whole time to the sorption apparatus.

Results and discussion

The starting compound for the post-synthetic modification (Cr-MIL-101-NH₂) was synthesized in a two-step procedure. First Cr-MIL-101-NO₂ was synthesized in a hydrothermal reaction starting from CrCl₃ and nitroterephthalic acid.²⁶ The dark green powder was washed and dried and, in the second step, the nitro groups were subsequently reduced with SnCl₂·2H₂O in EtOH. The light green powder was washed several times with H₂O and EtOH and dried in air. X-ray powder diffraction (XRPD) confirmed the purity of Cr-MIL-101-NO₂ and Cr-MIL-101-NH₂ (S1†).

The successful reduction of the nitro group was proven by IR spectroscopy. The asymmetric and symmetric NH₂- ($\nu = 3486$ and 3366 cm⁻¹) as well as the N–H-deformation ($\nu = 1586$ cm⁻¹) and the C–N-stretching ($\nu = 1256$ cm⁻¹) vibrations are clearly visible in the IR spectrum of Cr-MIL-101-NH₂ (S2†). Permanent porosity was demonstrated employing N₂ sorption measurements. The specific surface area and the micropore volume increased after the reduction of the NO₂ group, from $S_{\text{BET}} = 1687$ m² g⁻¹ and $V_{\text{m}} = 0.88$ cm³ g⁻¹ (at $p/p_0 = 0.5$) for Cr-MIL-101-NO₂ to $S_{\text{BET}} = 1850$ m² g⁻¹ and $V_{\text{m}} = 0.96$ cm³ g⁻¹ (at $p/p_0 = 0.5$) for Cr-MIL-101-NH₂ (S3†). The specific surface area was calculated from the BET-plot using the approach introduced by Rouquerol *et al.*³⁶

Post-synthetic modification was accomplished by treating the activated, evacuated Cr-MIL-101-NH₂ sample with the respective dye solution in a microwave oven. In order to accomplish the maximum *cis/trans* isomerisation, the degree of PSM, *i.e.* the available space per switch, was optimized. Therefore, four molar ratios BDC-NH₂²⁻ : dye = 2 : 1, 1.5 : 1, 1 : 1, and 1 : 2 were employed in order to vary the switch density. We are aware of the fact that we cannot predict the exact position of PSM (uniform functionalisation across the crystal). To ensure that no unreacted dye molecules are left within the pores, these were removed by washing with large amounts of ethanol. The modified Cr-MIL-101-NH₂ samples were characterized by XRPD measurements. Only reflections of the host compound were observed, though the relative reflection intensities changed due to the PSM with the dye molecules (S4†).

The correlation between the switch density and accessible porosity was established by N₂ sorption measurements (Table 2, S5†). As expected, higher switch densities lead to a decrease of the specific surface area and micropore volume. At molar ratios BDC-NH₂²⁻ : dye = 1 : 2 maximum functionalisation seems to be accomplished, but there are still free –NH₂ groups present in the sample as proven by NMR spectroscopy.

For further confirmation of the successful PSM of Cr-MIL-101-NH₂, IR- and NMR-spectroscopic investigations were carried out. IR spectra of the modified MOFs exhibit the characteristic bands of amide and urea groups. For Cr-MIL-101_{amide} three additional signals $\nu_{\text{C=O}} = 1668$ cm⁻¹, $\delta_{\text{N-H}} = 1508$ cm⁻¹ and $\nu_{\text{C-N}} = 1277$ cm⁻¹ are observed (Fig. 2). Accordingly two new signals $\nu_{\text{C=O}} = 1695$ cm⁻¹ and $\delta_{\text{N-H}} = 1543$ cm⁻¹ are found for Cr-MIL-101_{urea} (Fig. 3). These changes are accompanied by a decrease of the intensities ν_{NH_2} and $\nu_{\text{C-NH}_2}$ (data not shown).

Successful PSM is often demonstrated by dissolution of the modified MOF followed by NMR spectroscopic identification/characterization of the linker molecules.

Therefore, the Cr-MIL-101_amide and Cr-MIL-101_urea samples were decomposed by adding NaOH. After separation of Cr(OH)₃ by filtration and addition of HCl, a red and an orange

solid was obtained, respectively. The NMR spectra of these solids are shown in Fig. 4 and 5. The ¹H spectra of the extracted linker molecules exhibit signals due to aminoterephthalic acid (H₂BDC-NH₂), as well as the *cis* and *trans* isomers of the functionalized aminoterephthalic acid (H₂BDC-amide and H₂BDC-urea). One of the isomers is only present in small amounts.

Table 2 Specific surface areas S_{BET} and micropore volumes V_{m} of Cr-MIL-101_amide and Cr-MIL-101_urea

Molar ratio NH ₂ : dye	S_{BET} Cr-MIL-101_amide [m ² g ⁻¹]	V_{m} Cr-MIL-101_amide [cm ³ g ⁻¹]	S_{BET} Cr-MIL-101_urea [m ² g ⁻¹]	V_{m} Cr-MIL-101_urea [cm ³ g ⁻¹]
1 : 0	1850	0.96	1850	0.96
2 : 1	956	0.46	1194	0.58
1.5 : 1	898	0.43	948	0.46
1 : 1	800	0.38	847	0.43
1 : 2	792	0.37	733	0.36

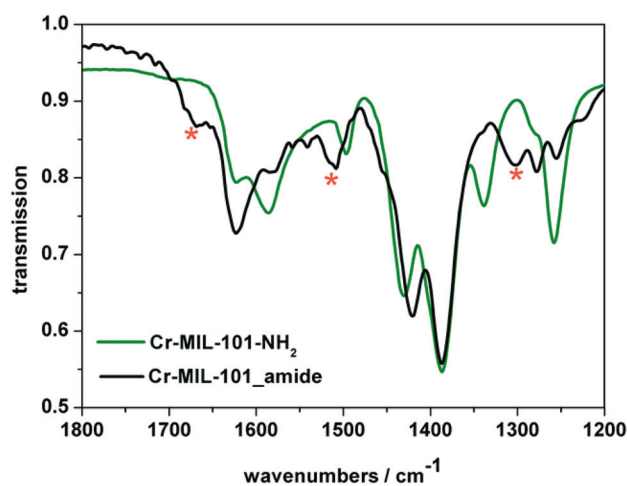


Fig. 2 IR spectra of Cr-MIL-101-NH₂ (green graph) and of Cr-MIL-101_amide (black graph). Characteristic amide-bands are marked by an asterisk.

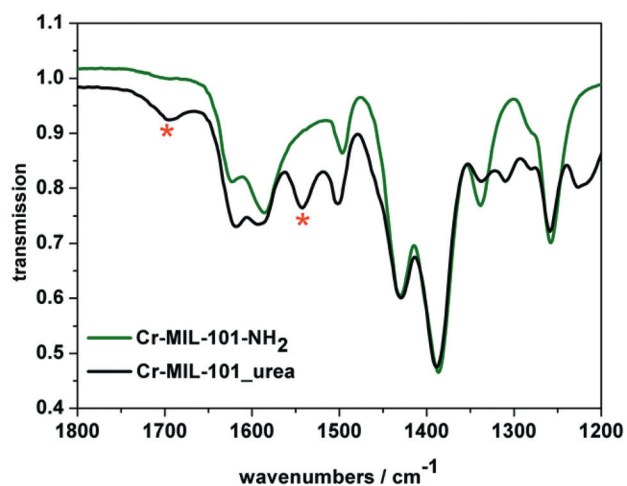


Fig. 3 IR spectra of Cr-MIL-101-NH₂ (green graph) and of Cr-MIL-101_urea (black graph). Characteristic urea-bands are marked by an asterisk.

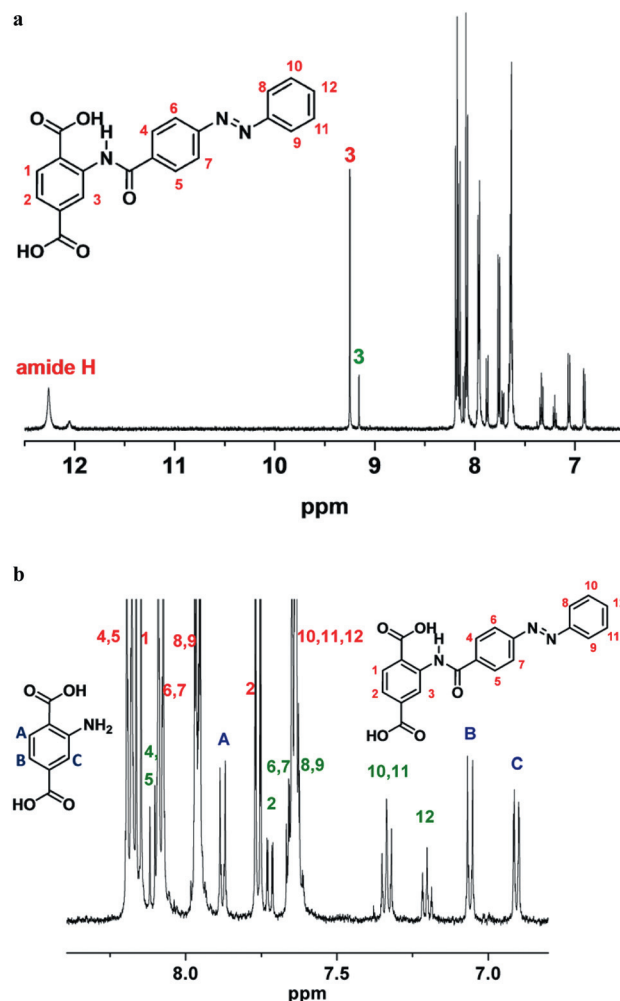


Fig. 4 (a) ¹H-NMR spectrum of H₂-BDC_amide (600 MHz, DMSO-d₆, 297 K, TMS): δ = 12.3 (s, 1H, H-amide), 9.25 (d, 1H, H-3), 8.18 (d, 2H, H-4, H-5), 8.15 (d, 1H, H-1), 8.08 (d, 2H, H-6, H-7), 7.96 (dd, 2H, H-8, H-9), 7.54 (dd, 1H, H-2), 7.63 (m, 3H, H-10, H-11, H-12) ppm. (b) ¹H-NMR spectrum of H₂-BDC_amide (600 MHz, DMSO-d₆, 297 K, TMS), red labels were assigned to the *trans*-H₂-BDC_amide and green labels to *cis*-H₂-BDC_amide protons, the protons of H₂-BDC-NH₂ are marked in blue.

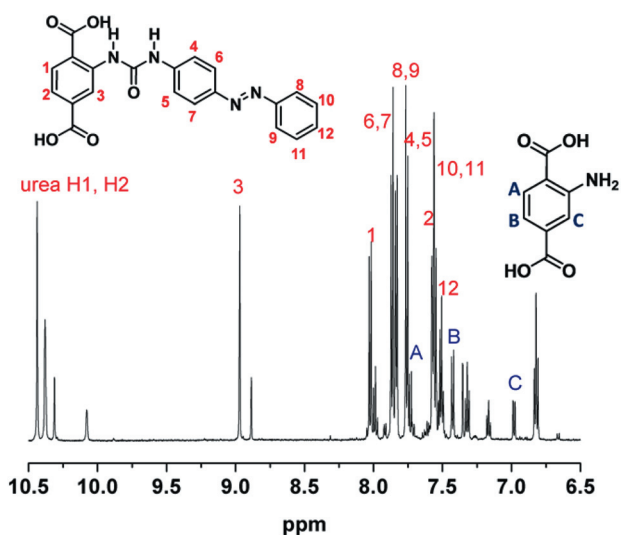


Fig. 5 ^1H -NMR spectrum of $\text{H}_2\text{-BDC}_{\text{urea}}$ (600 MHz, DMSO-d_6 , 298 K, TMS): δ = 10.43 (s, 1H, H-urea1), 10.38 (s, 1H, H-urea2), 8.97 (s, 1H, H-3), 8.0 (d, 1H, H-1), 7.86 (d, 2H, H-6, H-7), 7.84 (d, 2H, H-8, H-9), 7.76 (d, 2H, H-4, H-5), 7.58 (d, 1H, H-2), 7.56 (m, 2H, H-10, H-11), 7.51 (d, 1H, H-12) ppm.

The observed relative integrals of the ^1H signals correspond to the expected values. The signals were assigned using additional information from the HSQC-/HMBC- and COSY-NMR spectra (S6 and S7†). These results were confirmed by carrying out reference reactions using aminoterephthalate dimethyl ester instead of Cr-MIL-101- NH_2 . The ^1H -NMR spectra of the resulting products are almost identical to the ones obtained from the PSM of Cr-MIL-101- NH_2 (Fig. S8 and S9†). Photochemical isomerisation of the dye molecules and the functionalized Cr-MIL-101- NH_2 compounds was demonstrated by UV/Vis spectroscopy. The *cis/trans* isomerisation of the pure dye molecules was performed in solution and in a BaSO_4 matrix (S10 and S11†). Both dye molecules showed reversible *cis/trans* isomerisation in solution over several cycles, but no isomerisation reactions were observed in the BaSO_4 matrix. In solution both dye molecules exhibit distinct bands of each isomer (Fig. S10†). The bands at lower wavelength can be assigned to the $\pi \rightarrow \pi^*$ transition and at higher wavelength to the $n \rightarrow \pi^*$ transition of the azo-group. Upon irradiation with UV light, the intensity of the $\pi \rightarrow \pi^*$ transition decreases and the intensity of the $n \rightarrow \pi^*$ transition increases. The reversible back switching can be achieved using visible light or thermally.

To investigate the influence of the host-guest and guest-guest interactions on the switching efficiency, the switch density was varied. As determined by N_2 sorption experiments, the decrease of the molar ratios $\text{NH}_2 : \mathbf{1}$ or $\mathbf{2}$ in the PSM reaction from 2 : 1 to 1 : 2 leads to an increase of the linker densities (Fig. S5†, Table 1). At molar ratios $\text{BDC-NH}_2^{2-} : \text{dye} = 1 : 2$, maximum functionalisation is accomplished. Assuming a statistical distribution of the covalently attached dye molecules throughout the crystal, smaller linker densities should lead to more free space per molecule and thus less steric hindrance and therefore better switching properties. On the other hand, smaller switch densities will show a less pronounced change in the UV/Vis spectra due

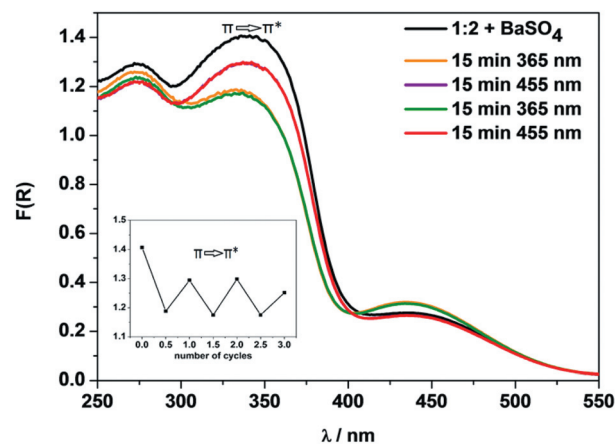


Fig. 6 Results of the UV/Vis switching experiment for Cr-MIL-101_amide (1 : 2).

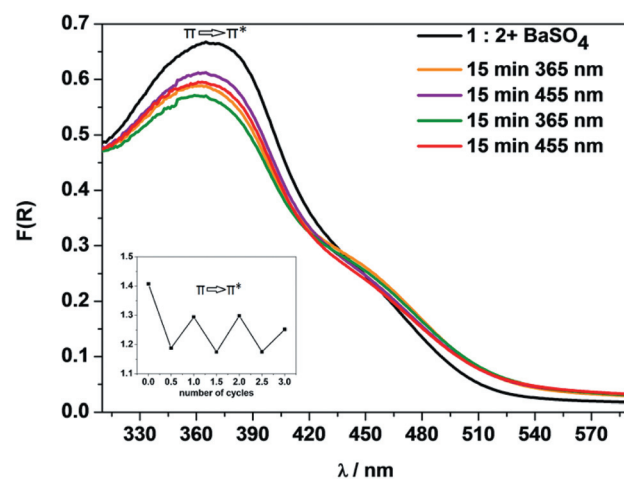


Fig. 7 Results of the UV/Vis switching experiment for Cr-MIL-101_urea (1 : 2).

to the lower concentration of chromophores. The UV/Vis spectra of all Cr-MIL-101_amide and Cr-MIL-101_urea compounds in a BaSO_4 matrix are presented in Fig. S12a-d and S13a-d†. Almost no influence of the switch density on the switching behaviour is observed. Samples with maximum functionalisation showed the most distinct switching behaviour (Fig. 6 and 7) in the UV spectra and were also used for the methane sorption experiments. All UV/Vis spectra show the characteristic changes in the band positions and intensities upon irradiation ($\lambda = 365 \text{ nm}$, 455 nm). In analogy to the linker molecules **1** and **2**, the band positions can be assigned to the $\pi \rightarrow \pi^*$ and $n \rightarrow \pi^*$ transitions of the *cis* and the *trans* products. The intensities of the $\pi \rightarrow \pi^*$ transitions were used for the qualitative evaluation. The pristine, well ground samples of Cr-MIL-101_amide and Cr-MIL-101_urea in the BaSO_4 matrix were alternately irradiated with UV ($\lambda = 365 \text{ nm}$) and Vis light ($\lambda = 455 \text{ nm}$) for 15 min.

For Cr-MIL-101_amide, irradiation with UV light ($\lambda = 365 \text{ nm}$) leads to an increase of the intensity of the band at $\lambda = 434 \text{ nm}$, while the intensity for the band at $\lambda = 335 \text{ nm}$ decreased

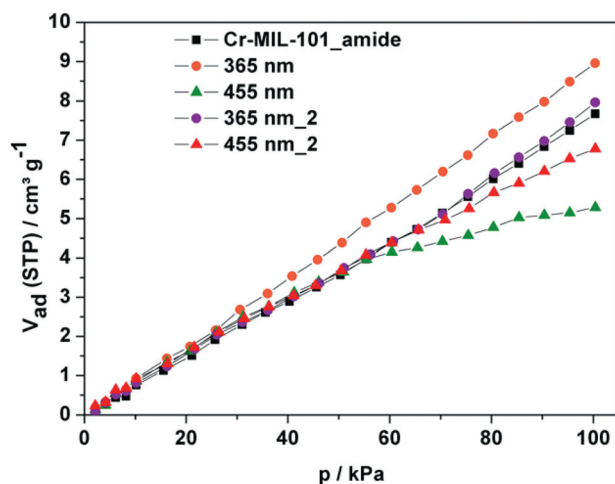


Fig. 8 Results of the methane sorption switching experiments for Cr-MIL-101_amide.

(Fig. 6). Back switching was achieved employing visible light. The intensity of the band at $\lambda = 434$ nm decreased and the intensity of the band at $\lambda = 335$ nm increased again, due to higher *trans*-isomer concentration. The results of repeated switching experiments are summarised in Fig. 6.

For Cr-MIL-101_urea, irradiation with UV light ($\lambda = 365$ nm) leads to a decrease of the intensity of the band at $\lambda = 363$ nm. Only small changes in the intensity of the band at $\lambda = 435$ nm are observed (Fig. 7). Back switching was achieved employing visible light. The intensity of the band at $\lambda = 363$ nm increased again, due to higher *trans*-isomer concentration. The results of repeated switching experiments are summarised in Fig. 7.

For both compounds Cr-MIL-101_amide and Cr-MIL-101_urea, only partial reversibility of the switching process is found. This phenomenon could be attributed to a photobleaching effect or to the steric hindrance of the switching process, the confinement effect. The strong influence of the host is confirmed by the observation that the *cis/trans* isomerization of the extracted PSM reaction products in solution is fully reversible (S14 and S15[†]).

Furthermore, we investigated the thermal back switching of the *cis*-isomer in Cr-MIL-101_amide and Cr-MIL-101_urea at room temperature. After irradiation with UV light the samples were left in the dark for 16 h, before the third UV/Vis spectrum was recorded (S16 and S17[†]). No or only small changes are observed for Cr-MIL-101_amide and Cr-MIL-101_urea, respectively. Therefore, large half-lives for the *cis/trans* isomerisation are expected and both compounds are suitable to investigate the sorption properties of the isomers.

Methane sorption experiments were carried out using Cr-MIL-101_amide and Cr-MIL-101_urea. Although only small changes are observed in the sorption isotherms, a general trend is clearly visible (Fig. 8 and 9). In both cases, the first sorption isotherm was recorded at 298 K after activation of the samples at 140 °C for 6 h. Subsequently the samples were again evacuated and irradiated for 90 min directly at the sorption instrument. Irradiation with UV light, *i.e.* increase of the *cis* isomer concentration, leads for both compounds to an increase in the CH₄ adsorption capacity. Irradiation with visible light results in a

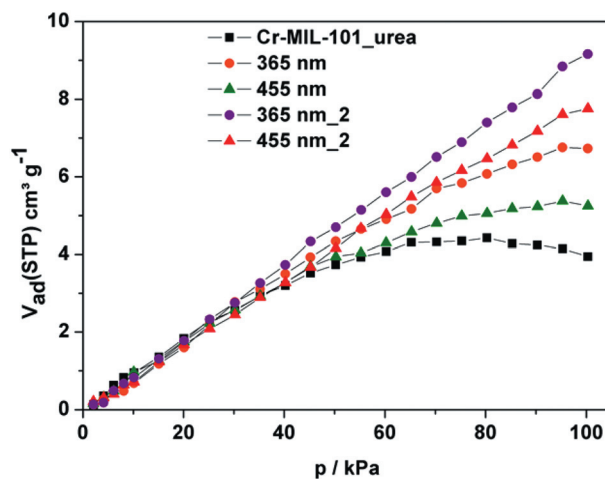


Fig. 9 Results of the methane sorption switching experiments for Cr-MIL-101_urea.

decrease of the maximally adsorbed amount of CH₄. This experiment was performed a second time with the same samples. As observed in the UV/Vis spectra, *cis/trans* isomerisation is not fully reversible and switching efficiency decreases over the number of switching cycles. This trend is confirmed by the CH₄ sorption isotherms of Cr-MIL-101_amide. For Cr-MIL-101_urea slightly different results are observed. Irradiation leads always to larger amounts of adsorbed CH₄ molecules. Nevertheless, alternating irradiation with UV/Vis light leads always to an increase/decrease in the sorption capacity, respectively.

The inclusion of azo-based switchable molecules has so far been accomplished using three different approaches. The adsorption of azobenzene in a flexible MOF has led to changes in the crystal structures.³⁷ The conformational change in the guest molecule upon irradiation triggers a structural transformation of the MOF and opens the pores for N₂ guest molecules. The use of azo-functionalized linker molecules for the synthesis of porous MOFs has also been reported.^{12,13,29} Although *cis/trans* isomerisation was clearly demonstrated only for the MOF-5 based system, differences in the CO₂ sorption behaviour were reported.²⁹ In the present paper, we have demonstrated that post-synthetic modification reactions can be used to introduce photo-switchable groups into MOFs. Reversible switching leads to small but distinct changes in the CH₄ sorption properties. Since there are only a limited number of systems containing photo-switchable azo-dyes, no general trends can be established. Large structural changes of the host upon *cis/trans* isomerisation seem to improve changes in the sorption properties substantially. Further work using rigid hosts will focus on the influence of the mode of attachment, the azo-dye and the use of other photo-switchable molecules.

Conclusions

In conclusion, we have shown that azo functionalized molecules can be introduced into MOFs by PSM. Different modes of attachment lead to different switching behaviour. Although *cis/trans* isomerization of the azo group has been demonstrated, the

effect is small and only partial reversibility is observed. These small changes lead also to variations in the CH₄ sorption behaviour.

Acknowledgements

This work has been supported by the State of Schleswig-Holstein and the Deutsche Forschungsgemeinschaft (DFG) via the SFB 677 *Function by Switching*. The authors thank Stephan Bernt for support in the synthesis of Cr-MIL-101-NH₂, Uschi Cornelissen and Stephanie Pehlke for supporting all spectroscopic measurements, the NMR-department for recording all NMR-spectra and Arne Klinkebiel for the help in the evaluation of the NMR-data.

Notes and references

- 1 R. E. Morris and P. S. Wheatly, *Angew. Chem., Int. Ed.*, 2008, **47**, 4966.
- 2 R. Babarao and J. Jiang, *Langmuir*, 2008, **24**, 6270.
- 3 A. U. Czaja, N. Trukhan and U. Mueller, *Chem. Soc. Rev.*, 2009, **38**, 1284.
- 4 U. Mueller, M. Schubert, F. Teich, H. Puetter, K. Schierle-Armdt and J. Pastré, *J. Mater. Chem.*, 2006, **16**, 626.
- 5 R. Babarao and J. Jiang, *J. Phys. Chem. C*, 2009, **113**, 18287.
- 6 Q. M. Wang, D. Shen, M. Bülow, M. L. Lau, S. Deng, F. R. Fitch, N. O. Lemcoff and J. Semanscin, *Microporous Mesoporous Mater.*, 2002, **55**, 217.
- 7 N. L. Rosi, M. Eddaoudi, J. Kim, M. O’Keeffe and O. M. Yaghi, *CrystEngComm*, 2002, **4**, 401.
- 8 M. Eddaoudi, J. Kim, D. Vodak, A. Sudik, J. Wachter, M. O’Keeffe and O. M. Yaghi, *Proc. Natl. Acad. Sci. U. S. A.*, 2002, **99**, 4900.
- 9 J. L. C. Rowsell and O. M. Yaghi, *Microporous Mesoporous Mater.*, 2004, **73**, 3.
- 10 A. Sonnauer, F. Hoffmann, M. Fröba, L. Kienle, V. Duppel, M. Thommes, C. Serre, G. Férey and N. Stock, *Angew. Chem., Int. Ed.*, 2009, **48**, 3791.
- 11 N. Stock and S. Biswas, *Chem. Rev.*, 2012, **112**, 933.
- 12 A. Modrow, D. Zargarani, R. Herges and N. Stock, *Dalton Trans.*, 2011, **40**, 4217.
- 13 S. Bernt, M. Feyand, A. Modrow, J. Wack, J. Senker and N. Stock, *Eur. J. Inorg. Chem.*, 2011, 5378.
- 14 S. M. Cohen, *Chem. Sci.*, 2010, **1**, 32.
- 15 S. M. Cohen, *Chem. Rev.*, 2012, **112**, 970.
- 16 M. Eddaoudi, J. Kim, N. Rosi, D. Vodak, J. Wachter, M. O’Keeffe and O. M. Yaghi, *Science*, 2002, **295**, 469.
- 17 H. Reinsch, M. Feyand, T. Ahnfeldt and N. Stock, *Dalton Trans.*, 2012, **41**, 4164.
- 18 S. Surblé, C. Serre, C. Mellot-Draznieks, F. Millange and G. Férey, *Chem. Commun.*, 2006, 284.
- 19 S. Biswas, T. Ahnfeldt and N. Stock, *Inorg. Chem.*, 2011, **50**, 9518.
- 20 Y. Goto, H. Sato, S. Shinkai and K. Sada, *J. Am. Chem. Soc.*, 2008, **130**, 14354.
- 21 T. Ahnfeldt, D. Gunzelmann, T. Loiseau, D. Hirsemann, J. Senker, G. Férey and N. Stock, *Inorg. Chem.*, 2009, **48**, 3057.
- 22 K. K. Tanabe and S. M. Cohen, *Angew. Chem., Int. Ed.*, 2009, **48**, 7424.
- 23 M. J. Ingleson, J. Perez Barrio, J.-B. Guilbaud, Y. Z. Khimyak and M. J. Rosseinsky, *Chem. Commun.*, 2008, 2680.
- 24 Z. Wang and S. M. Cohen, *Angew. Chem., Int. Ed.*, 2008, **47**, 4699.
- 25 Y. K. Hwang, D.-Y. Hong, J.-S. Chang, S. H. Jung, Y.-K. Seo, J. Kim, A. Vimont, M. Daturi, C. Serre and G. Férey, *Angew. Chem., Int. Ed.*, 2008, **47**, 4144.
- 26 S. Bernt, V. Guillermin, C. Serre and N. Stock, *Chem. Commun.*, 2011, **47**, 2838.
- 27 M. H. Mir, L. L. Koh, G. K. Tan and J. J. Vittal, *Angew. Chem., Int. Ed.*, 2010, **49**, 390.
- 28 D. Liu, Z.-G. Ren, H.-X. Li, J.-P. Lang, N.-Y. Li and B. F. Abrahams, *Angew. Chem., Int. Ed.*, 2010, **49**, 4767.
- 29 J. Park, D. Yuan, K. T. Pham, J.-R. Li, A. Yakovenko and H.-C. Zhou, *J. Am. Chem. Soc.*, 2012, **134**, 99.
- 30 K. M. Tait, J. A. Parkinson, S. P. Bates, W. J. Ebenezer and A. C. Jones, *J. Photochem. Photobiol., A*, 2003, **154**, 179.
- 31 J. Henzl, M. Mehlhorn, H. Gawronski, K.-H. Rieder and K. Morgenstern, *Angew. Chem., Int. Ed.*, 2006, **47**, 603.
- 32 H. Musterroph, R. Haessner and J. Epperlein, *J. Prakt. Chem.*, 1984, **326**, 259.
- 33 G. H. Coleman, G. Nichols, C. M. McCloskey and H. D. Ansporn, *Org. Synth.*, 1955, **3**, 712.
- 34 W. Siefgen, *Justus Liebigs Ann. Chem.*, 1948, **362**, 6.
- 35 L. C. Raiford and H. B. Freyermuth, *J. Org. Chem.*, 1943, **8**, 230.
- 36 J. Rouquerol, P. Llewellyn and F. Rouquerol, *Stud. Surf. Sci. Catal.*, 2007, **160**, 49.
- 37 N. Yanai, T. Uemura, M. Inoue, R. Matsuda, T. Fukushima, M. Tsujimoto, S. Isoda and S. Kitagawa, *J. Am. Chem. Soc.*, 2012, **134**, 4501.